STEM CELLS TRANSLATIONAL MEDICINE®

ENABLING TECHNOLOGIES FOR CELL-BASED CLINICAL TRANSLATION

# Efficacy and Safety of Immuno-Magnetically Sorted Smooth Muscle Progenitor Cells Derived from Human-Induced Pluripotent Stem Cells for Restoring Urethral Sphincter Function

YANHUI LI,[a,b*] MORGAINE GREEN,[a,c*] YAN WEN,[a] YI WEI,[a] PRACHI WANI,[a,c] ZHE WANG,[a,d] RENEE REIJO PERA,[e,f] BERTHA CHEN[a]

[a]Department of Obstetrics/Gynecology, Stanford University School of Medicine, California, USA; [b]Department of Obstetrics/Gynecology, Union Hospital, Tongji Medical College, Huazhong University of Science and Technology, The People's Republic of China; [c]Institute for Stem Cell Biology and Regenerative Medicine, Stanford University, California, USA; [d]Department of Obstetrics/Gynecology, NanFang Hospital, Southern Medical University, Guangzhou, Guangdong, The People's Republic of China; [e]Department of Cell Biology & Neuroscience; [f]Department of Chemistry and Biochemistry, Montana State University, Bozeman, Montana, USA

Correspondence: Yan Wen, M.D., Department of Obstetrics/Gynecology, HH333, Stanford University School of Medicine, Stanford, California 94305-5317, USA. Telephone: 650-723-9536; Fax: 650-723-7737; e-mail: yanwen@stanford.edu

*These authors contributed equally to this work and should be considered as co-first authors.

Received 6 April 2016; accepted for publication 31 October 2016; published Online First on 18 February 2017.


1066-5099/2017/$30.00/0

http://dx.doi.org/10.1002/sctm.16-0160



**Key Words.** Immunomagnetic separation • Flow cytometry • Myoblast, smooth muscle • Induced pluripotent stem cell • Urinary incontinence, stress • Elastin • Cell transplantation

## ABSTRACT

**Human-induced pluripotent stem cells (hiPSCs)-based cell therapy holds promise for treating stress urinary incontinence (SUI). However, safety concerns, especially tumorgenic potential of residual undifferentiated cells in hiPSC derivatives, are major barriers for its clinical translation. An efficient, fast and clinical-scale strategy for purifying committed cells is also required. Our previous studies demonstrated the regenerative effects of hiPSC-derived smooth muscle progenitor cells (pSMCs) on the injured urethral sphincter in SUI, but the differentiation protocol required fluorescence-activated cell sorting (FACS) which is not practical for autologous clinical applications. In this study, we examined the efficacy and safety of hiPSC-derived pSMC populations sorted by FDA-approved magnetic-activated cell sorting (MACS) using cell-surface marker CD34 for restoring urethral sphincter function. Although the heterogeneity of MACS-sorted pSMCs was higher than that of FACS-sorted pSMCs, the percentage of undifferentiated cells dramatically decreased after directed differentiation in vitro. In vivo studies demonstrated long-term cell integration and no tumor formation of MACS-sorted pSMCs after transplantation. Furthermore, transplantation of MACS-sorted pSMCs into immunodeficient SUI rats was comparable to transplantation with FACS-sorted pSMCs for restoration of the extracellular matrix metabolism and function of the urethral sphincter. In summary, purification of hiPSC derivatives using MACS sorting for CD34 expression represent an efficient approach for production of clinical-scale pSMCs for autologous stem cell therapy for regeneration of smooth muscle tissues.** STEM CELLS TRANSLATIONAL MEDICINE *2017;6:1158–1167*

## SIGNIFICANCE STATEMENT

This study provides a promisingly clinical-scale method for enriching committed cells from Human-induced pluripotent stem cells (hiPSCs) differentiation. Magnetic-activated cell sorting (MACS)-sorted smooth muscle progenitor cells (pSMCs) were heterogenous with negligible undifferentiated cells after in vitro directed differentiation. This cell population showed long-term tissue integration with no in vivo tumor formation. Furthermore, MACS-sorted pSMCs efficiently induced the remodeling of extracellular matrix of lower urinary tract and promoted functional recovery of the damaged urethra sphincter in a SUI animal model. These findings should facilitate translation of hiPSC-based cell therapy to clinical applications for smooth muscle regeneration.

## INTRODUCTION

Stress urinary incontinence (SUI) is the involuntary loss of urine during activities that increase intra-abdominal pressure, such as coughing, sneezing, laughing, lifting, and exercising [1]. SUI affects over 20% of the female population and is thought to be due to a combination of etiologies such as deficiencies in pelvic floor muscle and fascial support, and/or an incompetent urethral sphincter closure mechanism [2]. A significant risk factor for severe incontinence is childbirth injury and age-related atrophy of the urethral sphincter muscles [3]. SUI affecting men is often due to iatrogenic urethral sphincter injury from prostate surgery [4]. Current conservative treatment options of physiotherapy or periurethral injection of bulking agents provide only temporary relief with high recurrence rates [5]. Surgery is more effective, but

long-term recurrence is estimated to occur in approximately one out of five individuals, leaving a significant number of patients without adequate relief [6, 7]. Since the pathophysiology of SUI involves an incompetent urethral sphincter closure mechanism, likely due to injury or age-related loss of muscle cells in the urethral sphincter, therapeutic strategies that focus on regeneration of the damaged urethral muscle layers with stem/progenitor cells that can give rise to healthy muscle cells are particularly attractive. Various types of adult stem cells, isolated from bone marrow [8], skeletal muscle [9], and adipose tissue [10], have been tested for treatment of SUI in preclinical and clinical studies with encouraging results. However, adult stem cells are difficult to harvest and expand in vitro, especially in older patients. Therefore, alternate sources of early muscle progenitor cells are required for stem cell therapy to be clinically feasible.

Human-induced pluripotent stem cells (hiPSCs) were first generated in 2007 by the transfection of defined pluripotency factors [11, 12]. hiPSCs are derived from somatic cells of individual patients and enable an unlimited supply of autologous tissue and organ-specific cells via directed differentiation in vitro. Therefore, hiPSCs hold great promise for treating many debilitating human diseases [13, 14]. However, many challenges remain to be addressed prior to the clinical implementation of hiPSC-based therapies. One of these challenges is the lack of a clinical-scale method for purifying or enriching committed cells from a differentiated hiPSC cell population.

Differentiated cultures most frequently contain not only byproduct cells from multiple lineages, but also residual undifferentiated hiPSCs and/or differentiation-resistant cells [15]. The heterogeneity of differentiated cell population may affect the efficacy of cell transplantation. More worrisome is that undifferentiated cells may be tumorigenic after transplantation [16]. Hence, it is critical to eliminate the unwanted cells from the differentiated cell population that's destined for transplantation. Several purification strategies, such as serial passage [17], magnetic-activated cell sorting (MACS) [18], Percoll density gradient-based isolation[19], fluorescence-activated cell sorting (FACS) [20], genetically engineered cells carrying resistance or suicide genes[21], laser-mediated in situ cell purification [22], selective killing of undifferentiated human pluripotent stem cells (hPSCs) with a cytotoxic antibody[23], have been applied to generate nontumorigenic and homogenous cell populations. Of these, the only method that is currently approved by FDA for clinical purposes is MACS [24].

Various laboratories have reported efficient protocols for differentiation of hiPSCs into pSMCs through a population of FACS-sorted vascular progenitor cells (VPCs) [25, 26]. In vivo studies demonstrate that periurethral injection of hiPSC-derived pSMCs restores the structure and function of urethral sphincter in a SUI animal model [27, 28]. Nevertheless, these pSMCs were derived from FACS-sorted cells and FACS is not yet approved for cell separation in clinical applications of autologous cell therapies. Therefore, our objectives here were to investigate whether pSMCs can be induced from hiPSCs through a MACS-sorted intermediated cell population and whether the safety and efficacy of MACS-sorted pSMCs for treating SUI are comparable to FACS-sorted pSMCs.

## Materials and Methods

### Cell Culture and Differentiation

Institutional Review Board of the Stanford University School of Medicine and the Stanford University Stem Cell Research Oversight Committee approved this study. Written informed consents were obtained from all subjects. Two human-induced pluripotent stem cells (iPSC) cell lines, termed HuF5 and CAF, were investigated in this study. HuF5-iPSC line was reprogrammed from 46-year-old healthy female dermal fibroblasts via viral transduction of the transcription factors *Oct3/4, Sox2, Klf4, and c-Myc* [29] and was tagged with luciferase (Luc). CAF-iPSCs were derived from 50-year-old healthy female vaginal fibroblasts using nonintegrating episomal plasmids (Invitrogen, Carlsbad, CA, USA, http://www.invitrogen.com). iPSCs were maintained on matrigel-coated plates (BD Biosciences, San Diego, CA, USA, http://www.bdbiosciences.com) in mTeSR medium (StemCell Technologies, Vancouver, BC, Canada, http://www.stemcell.com). The protocol for VPCs and pSMC differentiation was adapted from Marchand et al. [25] and Wang et al. [30]. Briefly, iPSCs were passaged to Matrigel coated 10 cm plates at a final density of 10,000 cells per $cm^2$ in mTeSR supplemented with Y-27632 ROCk inhibitor (Cellagen Technology, San Diego, CA, USA, http://www.cellagentech. com). After 48–72 hours, the medium was replaced with chemically defined medium consisting of RPMI 1640 with 1 mM Glutamax, 1% w/v Nonessential Amino Acids (Invitrogen), 0.1 mM β-Mercaptoethanol, 1% w/v insulin-transferrin-selenium (Invitrogen) supplemented with 50 ng/ml of Activin A (PeproTech, Rocky Hill, NJ, USA, http://www.peprotech.com) and 50 ng/ml of human bone morphogenetic protein 4 (BMP4, PeproTech). For the following 8 days, the media was supplemented with 50 ng/ml fibroblast growth factor-2 (FGF-2, PeproTech) and 40 ng/ml of vascular endothelial growth factor (VEGF, Invitrogen). $CD34^+CD31^+$ VPCs and $CD34^+$ intermediate cells were sorted by fluorescently activated or MACS, respectively, on day 10 of differentiation, and then plated on collagen IV coated plates at a density of 50,000 cells per $cm^2$ in smooth muscle growth medium (SMGS, Invitrogen) supplemented with PDGF-BB (10 ng/ml) for 14 days. The cells were passed every 5 days or at 90% confluency.

### Fluorescence-Activated or Magnetic-Activated Sorting of Vascular Progenitor Cell

After treated with 10-μM Rock inhibitor for 30 minutes, differentiated cells were dissociated with 0.05% w/v Trypsin–EDTA (Thermo scientific, Fremont, CA, USA, http://www.thermoscientific.com), and then passed through a 70 μM filter to ensure a single cell solution. Dissociated cells were resuspended in a small volume of fetal bovine serum (FBS) and placed in incubator for 30 minutes for recuperation. After recuperation, cells were resuspended in sorting buffer (phosphate-buffered saline [PBS] + 0.5% w/v FBS min + 2 mM EDTA), counted, and prepared for either MACS or FACS. FACS was used as comparison.

For MACS, cells were first immuno-labeled with CD34 microbeads (Miltenyi Biotec, Auburn, CA, USA http://www.miltenyibiotec.com/). Magnetic labeling was performed strictly according to the manufacturer's instructions. In brief, after centrifuge, the cell pellet was re-suspended in 300 μl precooled sorting buffer for up to $10^8$ total cells. Then 100 μl of FcR Blocking Reagent (Miltenyi Biotec) and 100 μl of CD34 MicroBeads were added and incubated at 2°C–8°C for 30 minutes. The cells were washed with 5 ml of sorting buffer. The cells were resuspended in 500 μl of

sorting buffer. Magnetic separation was proceeded using an autoMACS pro Separator (Miltenyi Biotec). The magnetically labeled $CD34^+$ VPCs were obtained by positive selection and directly taken into culture or analyzed for purity by flow cytometry.

For FACS, cells were blocked with mouse IgG (R&D Systems Inc., Minneapolis, MN, USA, http://www.rndsystems.com) for 15 minutes and stained with FITC Mouse Anti-Human CD31 and PerCP-Cy5.5 Mouse Anti-Human 34 (BD Biosciences) for 30 minutes. Stained cells were washed with sorting buffer and spun down at 1,000 g for 5 minutes. Pellets were resuspended in 1 ml sorting buffer for sorting. $CD31^+CD34^+$ cells were sorted on a FACS Aria II (BD Biosciences) and checked for purity.

### Immunofluorescent Staining

Cells were fixed in 4% v/v paraformaldehyde for 10 minutes and washed three times with 0.1% v/v Tween-20/PBS. Cells were permeabilized 1% v/v TritonX-100 for 30 minutes at room temperature and then blocked using Serum Free Protein blocker (Gibco) for an additional 30 minutes. Cells were incubated with primary antibodies for $\alpha$-SMA (1:200, mouse monoclonal antibody, Abcam Inc., Cambridge, MA, USA, http://www.abcam.com), SM-22 (1:50, goat polyclonal antibody, Abcam), TRA1-60 (1:200; mouse polyclonal antibody, EMD Millipore Corporation, Temecula, CA, USA, http://www.emdmillipore.com), and Ki-67 (1:100; mouse monoclonal antibody, BD Bioscience) overnight at 4°C. To remove excess primary antibody, the cells were washed three times with 0.1% v/v Tween-20/PBS and then incubated with secondary antibody as following: Alexa 488-conjugated anti-mouse IgG (1:300, Invitrogen), and Alexa 594-conjugated anti-goat IgG (1:300, Invitrogen) for 1 hour at room temperature. The cells were washed again, and then counterstained with DAPI before imaging on a Zeiss Axioplan 2 Imaging microscopy (Jena, Germany, http://www.zeiss.com). Negative controls were performed by deletion of the primary antibody from antibody dilution buffer.

### Animal Care and Generation of SUI Rat Model

Female immunodeficient Rowett Nude rats (RNU, Charles River Laboratories, Hollister, CA, USA, http://www.criver.com/) weighing 200–250 g were used to investigate the effects of pSMCs on urethral sphincter function. Eight to ten-week-old CB17 SCID female mice (Charles River Laboratories) were utilized to examine the long-term (6 months) in vivo survival and for safety testing (in vivo teratoma formation) of pSMCs. All animals were maintained at the Stanford University Research Animal Facility in accordance with Stanford University's Institutional Animal Care and Use Committee guidelines. Animal experiments were approved by the Institutional Review Board of the Stanford University School of Medicine and the Stanford Administrative Panel of Laboratory Animal Care (APLAC).

A rat model of SUI was established via transabdominal urethrolysis as described by Rodriguez et al. [31]. This SUI rat model showed significantly decreased urethral resistance and urethral smooth muscle damage for at least 8 weeks after surgery [32], therefore it is an appropriate animal model for studying smooth muscle regeneration in cell therapy [33]. Our studies also confirmed the published data on persistence of SUI for at least 8 weeks (unpublished data). This is why the efficacy experiments were terminated 8 weeks after urethrolysis surgery. Beyond this point, the SUI condition may spontaneously resolve in rodents. Since we previously documented that extracellular matrix (ECM) in pelvic connective tissue from women with SUI is modulated by cyclic reproductive hormones [34], and the majority of SUI patients who may require stem cell therapy are older and likely to be estrogen deficient, we also performed bilateral ovariectomy on the rodents to eliminate the influence of estrus cycle on the ECM metabolism and to simulate an estrogen-deficiency state [35].

In brief, RNU rats were intraperitoneally anesthetized with ketamine (30 mg/kg) and xylazine (3 mg/kg). The ovaries were exteriorized through a lower abdominal incision. After ovarian vessels were ligated, bilateral ovaries were excised. The bladder and urethra were identified and circumferentially separated from anterior vaginal wall and pubic bone by sharp dissection, thus causing injury to the urethral sphincter. The abdominal skin was closed with wound clips. The animal was monitored until recovery.

### Cell Injection and Tissue Collection

The rats were randomly divided into three groups: 1. urethrolysis plus mixture of saline and SMGS medium injection (sham-saline group, $n = 16$), 2. urethrolysis plus MACS-sorted CAF-pSMC injection (MACS-CAF-pSMC group, $n = 11$), 3. urethrolysis plus FACS-sorted CAF-pSMC injection (FACS-CAF-pSMC group, $n = 9$). pSMCs were injected at passage 4. Three weeks after urethrolysis (after healing from the urethrolysis surgery), the cells or saline mixed with medium were injected periurethrally. The rats were anesthetized with 3–4% v/v isoflurane and a total of $2 \times 10^6$ cells suspended in 100 μl SMGS medium were injected periurethrally at two sites using a 28.5-gauge insulin syringe. SUI rats in the sham-saline group underwent injections with 50 μl SMGS medium mixed with 50 μl of saline only (to simulate cell suspension). The amount of SMGS in the injection for the sham-saline group was reduced in order to keep all injection volumes at 100 μl. This was done in order to reduce bias from the operators performing the injections and urethral pressure testing. Researchers were blinded to the treatment group allocations. In vivo bioluminescence imaging (BLI) was used to track and monitor the transplanted cells, as described in our previous publication [27]. The rat urethras and bladders were collected 5 weeks after injection, upon euthanasia after leak point pressure (LPP) testing.

For the long-term cell integration and safety study, SCID mice ($n = 10$), $1 \times 10^6$ pSMCs in 50 μl of Matrigel (50% w/v) were injected directly into the adductor longus muscles to monitor for long-term tumor formation, as described by Hentze et al. [17]. After 6 months of monitoring, the mice were sacrificed and the hind leg skeletal muscles harvested, embedded in Tissue-Tek O.C.T. compound (Sakura Finetek, Tokyo, Japan, http://www.sakura-finetek.com) and stored at −80°C for further studies.

### In Vivo BLI of Transplanted pSMCs

For in vivo cell tracking of the transplanted pSMCs, Luc-tagged and MACS-sorted HuF5-pSMCs were injected into the hind legs of SCID mice ($n = 10$). Transplanted cell survival was monitored via BLI using the Xenogen in vivo Imaging System (Caliper Life Sciences, Waltham, MA, USA, http://www.perkinelmer.com). Briefly, luciferase substrate D-luciferin (Biosynth, Itasca, IL, USA, https://www.biosynth.com) was administered intraperitoneally (150 mg/kg) 15 minutes prior to image acquisition. Animals were placed in a light-tight chamber, and photons emitted from luciferase-expressing cells were collected with integration times of 2 minutes. BLI signal was quantified in maximum photons per second per $cm^2$ per steradian and presented as $Log_{10}$ (photons per second). Images were obtained every week for 6 months.

### Leak Point Pressure Measurement

The LPP measurement was used to assess urethral muscle function in sham-saline and cell-treated rats, and LPP were performed as described by Conway et al. [36]. Investigators performing LPP measurement were blinded to the group assignment of each animal. Briefly, 5 weeks after cells or culture medium injection, the rats were anesthetized with ketamine (30 mg/kg) and xylazine (3 mg/kg). A transvesical catheter with a fire-flared tip was inserted into the bladder dome through a small abdominal incision. The abdominal wall was closed, and the catheter was connected via a three-way stopcock to a 50-ml syringe for filling with methylene blue colored saline and to a pressure transducer (TSD 104A, BIOPAC Systems Inc., CA, USA, http://www.biopac.com) for monitoring bladder pressure. The bladder pressure was amplified and sampled by a biological signal acquisition system (BIOPAC MP 150) and digitalized for computer data collection using Acqknowledge acquisition and analysis software (BIOPAC Systems Inc.).

Before LPP testing, the spinal cord was transected at the T8-T10 level to eliminate the voiding reflex mediated by spinobulbospinal pathways. The urethral closure mechanism during urine storage remains intact because urethral contractile reflexes activated by sympathetic and somatic nerves responding to bladder distension are predominantly organized at the lumbosacral spinal cord level. The vertical tilt table/intravesical pressure clamp model was used to measure the LPP (Supporting Information Fig. 1). The rat is taped to a board and placed in the vertical position. The 50-ml syringe (reservoir) which is connected to the bladder catheter via the three-way stopcock was then fixed onto a metered vertical pole. Bladder filling was done by manually raising the height of the reservoir by 2–3 cm increments for every 2 minutes starting from 0 cm, until urinary leakage (methylene blue saline) was observed at the urethral meatus. The bladder pressure (measured by the transducer) at which leakage was observed was recorded as the LPP. The pressure at which leakage occurred was defined as the LPP. LPP is thus a measure of the urethral sphincter pressure against bladder filling. The mean of at least three consecutive LPPs was taken as a data point for each animal.

### Histological Analysis

To examine for tumor formation or abnormal histology, the adductor longus muscles of SCID mouse were excised and fixed with 10% buffered formalin phosphate solution for 16 hours. Paraffin-embedded specimens were cut into 5-μm sections, and hematoxylin and eosin staining was performed. The slides were detected by light microscope.

### RNA Extraction and Real Time Quantitative Polymerase Chain Reaction (PCR)

Total RNA was isolated using the RNeasy mini kit (Qiagen, Hilden, Germany, http://www.qiagen.com) and reverse-transcribed into cDNA with using the M-MLV reverse transcriptase system (Thermo scientific). Brilliant SYBR Green QPCR Master Mix (Stratagene, La Jolla, CA, USA, http://www.genomics.agilent. com) was used to perform PCR. PCR primers used to amplify *Oct4, Sox2, SMTN, ACTA1 and GAPDH* are shown in Table 1. GAPDH was used as an endogenous reference. Gene expression analysis was performed using Mx3005P Multiplex Quantitative PCR System with MxPro QPCR software (Stratagene, La Jolla, CA, USA). Samples were analysed in duplicate and their geometric mean calculated for normalization to the housekeeping GAPDH gene.

**Table 1.** Primers used for real-time quantitative reverse transcription PCR

| Gene | Strand | 5′–3′ sequence | Accession numbers |
|---|---|---|---|
| *GAPDH* | Sense | CTCAACGACCACTTTGTCAAGCTCA | NC_000012.12 |
| | Anti-sense | GGTCTTACTCCTTGGAGGCCATGTG | |
| *Oct4* | Sense | TCGAGAACCGAGTGAGAGG | NC_000006.12 |
| | Anti-sense | GAACCACACTCGGACCACA | |
| *Sox2* | Sense | AGCTACAGCATGATGCAGGA | NC_000069.6 |
| | Anti-sense | GGTCATGGAGTTGTACTGCA | |
| *SMTN* | Sense | TTGGACAAGATGCTGGATCA | NC_000022.11 |
| | Anti-sense | CGCTGGTCTCTCTTCCTTTG | |
| *ACTA1* | Sense | CCAGTGTGGAGCAGCCCAGC | NC_000001.11 |
| | Anti-sense | TCACCCCCTGATGTCTGGGACG | |

GenBank accession numbers indicate transcript variants with homologous sequences to primers.

### Western-Blot Analysis

Rat urethras and bladders were cut into small pieces and homogenized on ice with a RIPA buffer (50 mM Tris, 150 mM NaCl, 1% NP40, 0.5% deoxycholate, 0.1%SDS, 4 mM EDTA, and 2 mM PMSF, pH 7.4). Total protein concentrations were determined using the Bradford method (Bio-Rad, Hercules, CA, USA, http://www.bio-rad.com/). The samples were not reduced for analysis of collagen proteins and reduced for analysis of elastin protein with a sodium dodecyl sulfate (SDS) sample buffer containing 5% w/v of 2-mercaptoethanol and boiled for 10 minutes. Samples (70 μg per lane) were subjected to 8% polyacrylamide gels (SDS-PAGE, Bio-Rad). The gels were blotted onto nitrocellulose membranes (Bio-Rad) in an electrophoretic transfer cell. After blocked with 5% v/v nonfat milk, the blots were probed with goat anti-rat α-elastin (1:500, Abcam Inc., Cambridge, MA, USA, http://www.abcam.com) at room temperature for 1 hour or mouse anti-rat collagen III (1:500, Abcam Inc.) at 4°C overnight. After washing three times with phosphate buffered saline with 0.1% v/v Triton (PBS-T), the membrane was then incubated with HRP conjugated mouse anti-goat IgG (1:50,000, GE Healthcare, Pittsburgh, PA, USA, http://www.gelifesciences.com) and sheep anti-mouse IgG (1:2,000, GE Healthcare) for 1 hour at room temperature. The blots were washed with PBS-T three times, developed by chemiluminescence, and re-probed with rabbit anti-GAPDH polyclonal antibody (1/2,000, Abcam, Inc), then 1/10,000 dilution of donkey anti-rabbit IgG conjugated to HRP (GE Healthcare). The relative densities of bands were assessed using ImageJ Version 1.48 (NIH).

### Statistical Analysis

Statistical analyses were performed using SPSS version 21 (SPSS Inc., Chicago, IL, USA, http://www-01.ibm.com/software/analytics/spss/). Results are expressed as means ± SEM. Kruskal-Wallis one way *ANOVA* on ranks followed by Wilcoxon-Mann-Whitney test were used to compare variables. A value of $p < .05$ was considered significant.

## Results

### Purification of hiPSC Derivatives to Further Differentiate into pSMCs

To examine the relative purities of VPCs within the unsorted, MACS-sorted, and FACS-sorted populations, FACs analysis of each population was conducted immediately after harvesting or

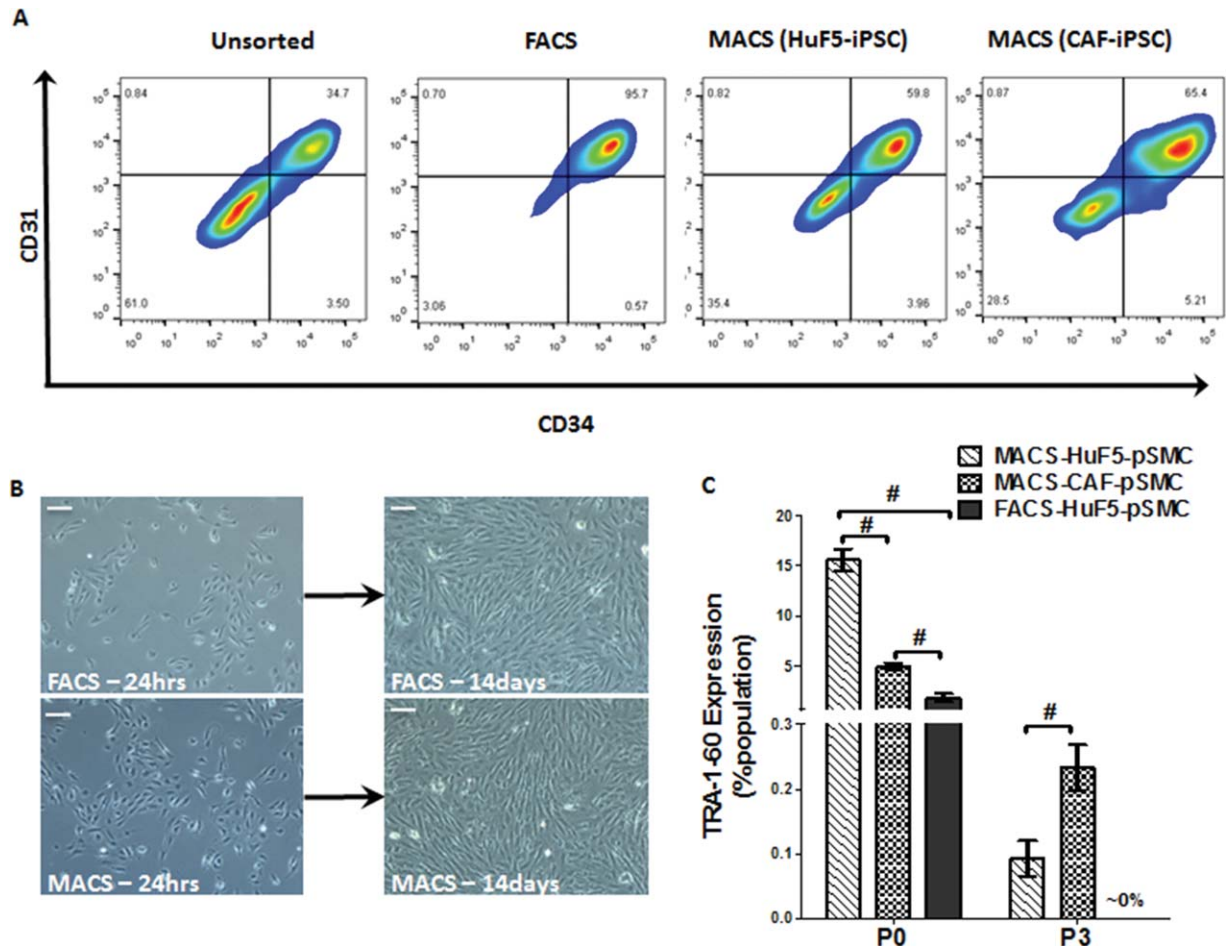


**Figure 1.** Comparative fluorescence-activated cell sorting (FACS) analysis of sorting methods**. (A)**: Representative graphs for FACs analysis of the percentage of $CD31^+CD34^+$ vascular progenitor cells (VPCs) in unsorted HuF5-induced pluripotent stem cells (iPSC) derivatives, FACS-sorted (HuF5-iPSCs), and magnetic-activated cell sorting (MACS)-sorted (HuF5-iPSC and CAF-iPSCs) intermediate cell population at passage 0. **(B)**: Representative bright-field images of FACS and MACS populations from 24 post hours (VPCs) and 14 days post sorting (smooth muscle progenitor cells). Scale bar, 200 μm. **(C)**: Average TRA-1-60 expression from FACS analysis at 0 days and 14 days for the FACS and MACS populations. Error bar indicates mean ± standard error of mean ($n \geq 3$). $^{\#}p < .05$ by Mann-Whitney test. Abbreviations: FACS, fluorescence-activated cell sorting; iPSCs, induced pluripotent stem cells; MACS, magnetic-activated cell sorting; pSMCs, smooth muscle progenitor cells.

sorting. In triplicate runs, the average percentage of $CD31^+CD34^+$ VPC populations were 33.9% ± 2.34% in unsorted HuF5-iPSC derivatives, 58.5% ± 10.75% in MACS-sorted HuF5-iPSC intermediate cell population, 65.4% ± 8.24% in MACS-sorted CAF-iPSC intermediate cell population and 95.8% ± 0.61% in FACS-sorted HuF5-iPSC intermediate cell population (Fig. 1A**)**. After cultured in SMGS media for 14 days, both MACS-sorted and FACS-sorted cells exhibited the characteristic "spindle" appearance of SMC **(**Fig. 1B**).**

The change in TRA-1-60 (a well characterized pluripotent cell surface marker) was analyzed in both the MACS and FACS populations from the initial sort to the third passage. Initially, the percentage of TRA-160 positive cells in the MACS sorted population was significantly higher than that in FACS-sorted HuF5-VPC population (MACS-HuF5: 15.60% ± 2.43% and MACS-CAF: 4.93% ± 0.55% vs. FACS-HuF5: 1.81% ± 0.71%; $p < .05$, respectively). However, between p0 and p3, expression of this pluripotency marker dropped dramatically in the MACS population (HuF5-pSMCs: 0.09% ± 0.05% and CAF-pSMCs: 0.30% ± 0.06%), suggesting that culture conditions and passaging assisted in the selection process (Fig. 1C).

## Characterization of the pSMCs Derived from MACS-Sorted and FACS-Sorted VPCs

To compare the expression patterns of the sorted populations, the cells were analyzed for the expression of the myogenic proteins αSMA, SM-22α, and TRA-1-60. Both MACS and FACS populations stained positively for αSMA and SM-22α in all cells observed. Ki-67, a marker of proliferation, was positive for MACS- and FACS-sorted cells, consistent with progenitor cell behavior. TRA-1-60 positive cells were not detected by visual inspection (Fig. 2). mRNA levels of pluripotent markers Oct4 and Sox-2 showed decreasing trends in MACS-sorted CAF-iPSC-pSMCs after serial passage, while smoothelin gene expression, a smooth muscle cell protein, showed an increasing trend (data not shown). Statistical analysis of the PCR data was not possible due to small sample size in triplicate preparations.

## MACS-Sorted pSMCs Survived In Vivo and Showed No Risk of Teratoma Formation

To address potential safety issues regarding the mixed population in MACs sorted cells, $1 \times 10^6$ cells were injected into the hind leg

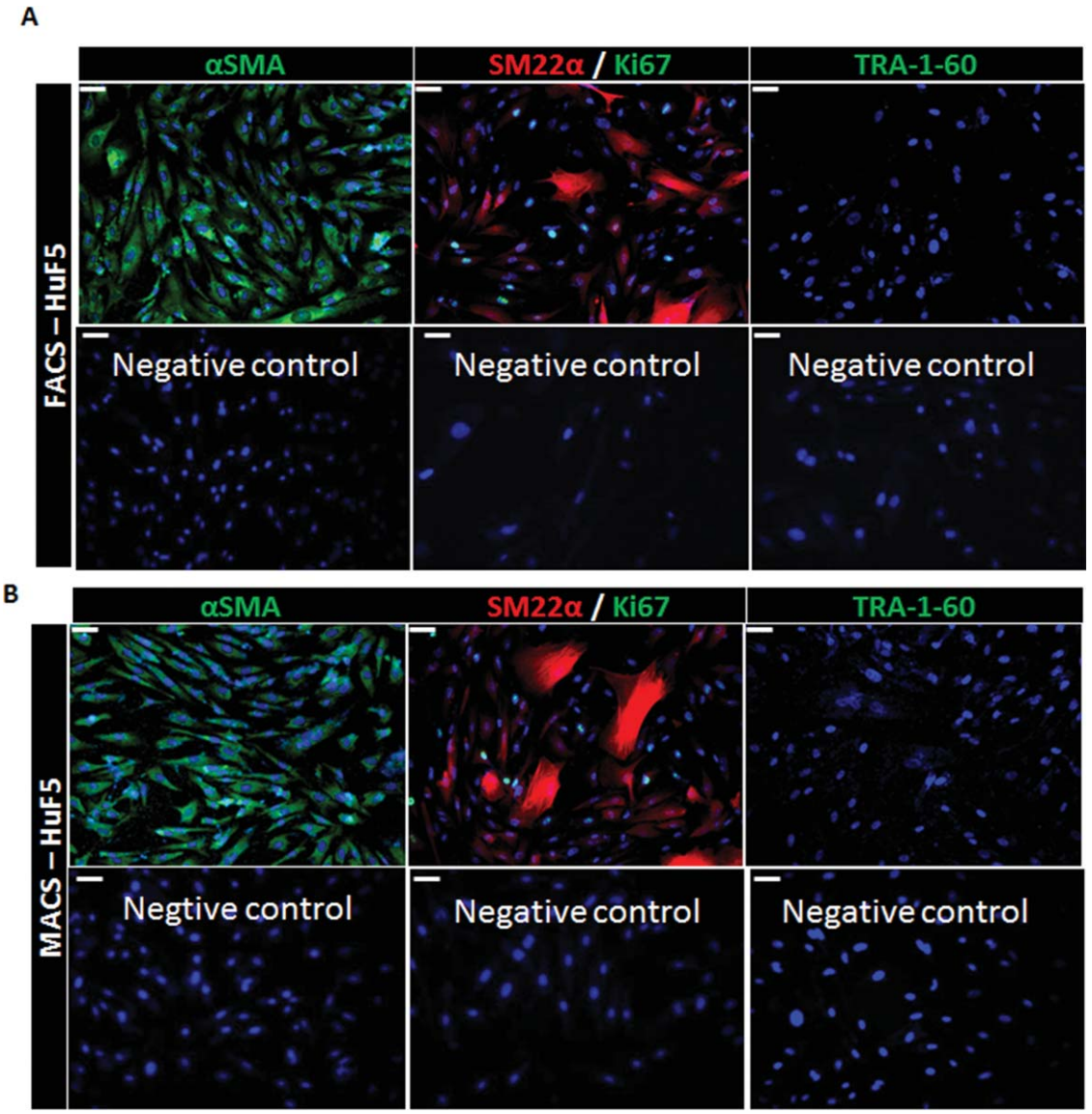


**Figure 2.** Characterization of the smooth muscle progenitor cells (pSMCs) Derived from magnetic-activated cell sorting (MACS)-sorted and fluorescence-activated cell sorting (FACS)-sorted vascular progenitor cells (VPCs). Immunofluorescence staining showed that most of pSMCs derived from FACS-sorted VPCs **(A)** and MACS-sorted VPCs **(B)** were positively stained for αSMA (green), SM-22 (red), and ki-67 (green), but negatively stained for the pluripotent marker TRA-1-60 (green). The bottom rows of (A) and (B) are representative images from negative controls. Scale bar, 200 μm. Abbreviations: FACS, fluorescence-activated cell sorting; MACS, magnetic-activated cell sorting.

of ten SCID mice and monitored over the course of 6 months with BLI. During this time, the BLI signal intensity decreased and was eventually lost in 8 out of 10 mice, 2 showed persistent BLI signals (Fig. 3A). While no outward signs of teratoma presented, all hind leg tissues were stained and examined. No abnormal histology or teratomas were observed (Fig. 3B), even in the BLI positive tissues. The observation of BLI signal over such a long period of time (6 months) without an increase in signal or detection of anomalous cells suggests engraftment without formation of harmful tissues.

## MACS-Sorted and FACS-Sorted pSMCs Provide Similar Therapeutic Effects on the Injured Urethra

Compared with intact rats (no surgery and no treatment) in our previous studies [27], mean LPP was significantly lower in saline-injected SUI rats 8 weeks after urethrolysis (13.94 $\pm$ 4.07 cm $H_2O$ vs. 17.67 $\pm$ 1.11 cm $H_2O$ [27], $p < .05$), indicative of decreased function of the urethral sphincter. LPP in SUI rats that underwent periurethral injection of MACS-sorted pSMCs was significantly higher than saline-treated rats (19.15 $\pm$ 3.70 cm $H_2O$ vs. 13.94 $\pm$ 4.07 cm $H_2O$, $p < .05$), demonstrating that MACS-sorted pSMCs facilitated the recovery of urethral function. It is noteworthy that there was no difference in the increase of mean LPP between MACS-sorted and FACS-sorted pSMC-treated rats (19.15 $\pm$ 3.70 cm $H_2O$ vs. 19.40 $\pm$ 5.94 cm $H_2O$, $p > .05$), indicating that both pSMC populations have similar therapeutic effect on the injured rat urethra **(**Fig. 4**)**.

## MACS-Sorted pSMCs Induced ECM Remodeling in Rat Lower Urinary Tract

We previously documented that alteration of ECM components in the lower urinary tract after urethrolysis may contribute to the

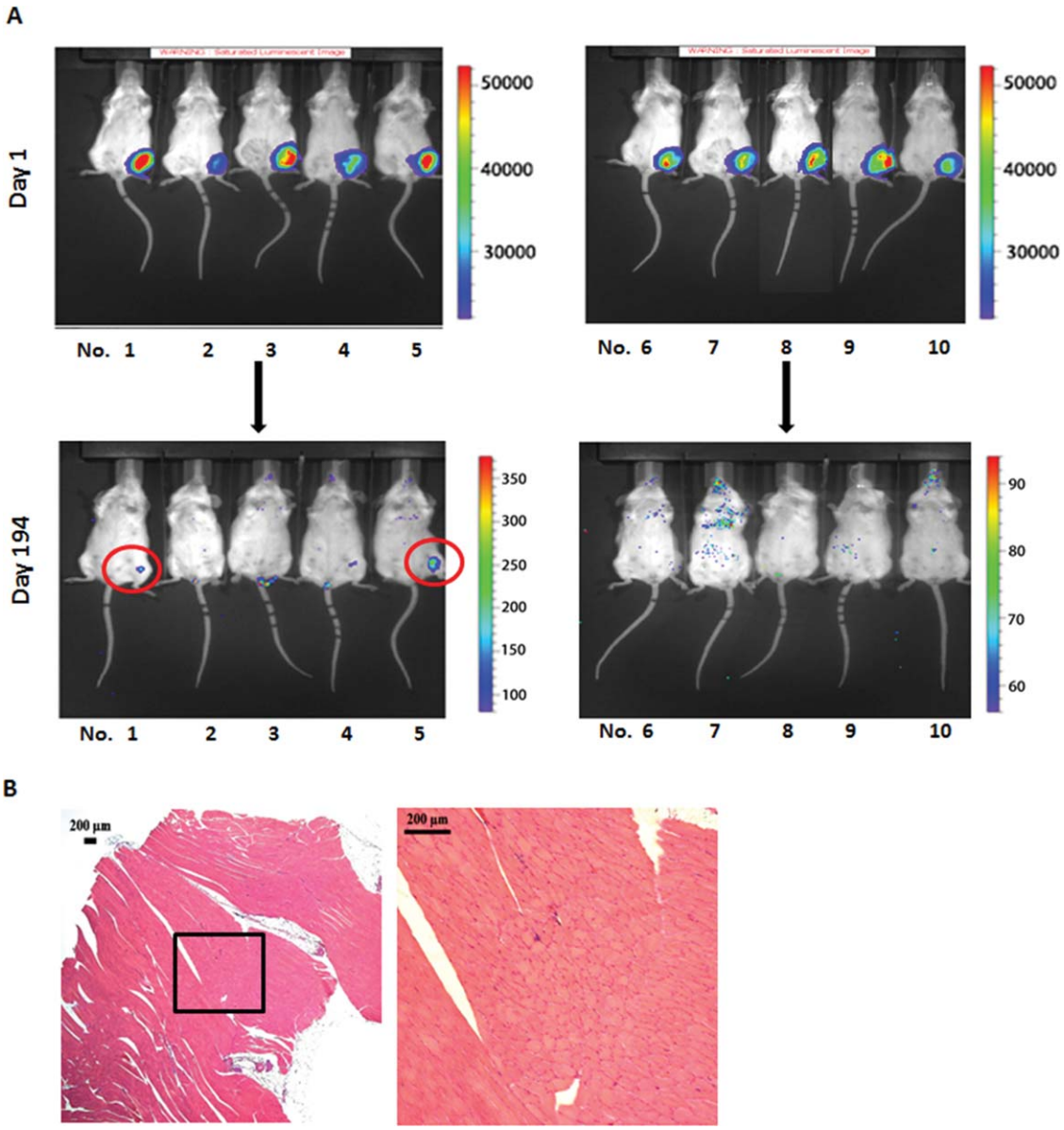


**Figure 3.** In vivo survival study and teratoma assay of transplanted smooth muscle progenitor cells (pSMCs) in SCID mice. **(A)**: In vivo tracking of transplanted luciferase-tagged-HuF5-pSMCs with bioluminescent imaging (BLI). To assess longitudinal cell survival in vivo, SCID mice were continuously monitored. Two mice still exhibit weak BLI signal at 194 days post cell transplantation. **(B)**: Tissue section analysis showed that no teratoma formation in the injected mouse hind leg muscles sites at 194 days after HuF5-pSMC injection. Representative H&E-stained images are shown. Scale bar, 200 μm.

occurrence of urine incontinence in SUI rats and transplantation of FACS-sorted pSMCs can efficiently promote the recovery of damaged urethral sphincter through induction of elastogenesis [28]. To document the effect of MACS-sorted pSMCs on the ECM remodeling of rat lower urinary tract, we examined the expression of elastin and collagen III proteins in the rat urethra and bladder. Consistent with our previous studies, FACS-sorted CAF-pSMC-treated rats also displayed increasing trend in the elastin content in rat bladder compared to the sham-saline group, although the difference was not significant (Fig. 5A). The protein level of elastin in rat bladders from the MACS-CAF-pSMC group was significantly higher than the sham-saline group ($p < .01$), suggesting that injection of MACS-sorted pSMCs induced the elastogenesis in the injured lower urinary tract **(**Fig. 5B**)**. No significant difference in the expression of collagen-III protein was observed between MACS-CAF-pSMC group and sham-saline group.

## Discussion

In this study, we demonstrated that human pSMCs can be efficiently induced from MACS-sorted $CD34^+$ intermediate cell population. After directed differentiation in vitro, these $CD34^+$ cell-derived pSMCs were positively stained with specific myogenic markers and contained very low levels of TRA-1-60 positive cells. In vivo studies showed the long-term survival of these cells and no signs of teratoma formation or abnormal histology after transplantation. Furthermore, periurethral injection of pSMCs derived from MACS-sorted $CD34^+$ cells, similar to the FACS-sorted pSMCs,

efficiently induced elastogenesis in the lower urinary tract and promoted functional recovery of the damaged urethral sphincter in immunodeficient SUI rats.pSMCs derived from hiPSCs showed promise for treating SUI [27]. However, difficulty in controlling the heterogeneous nature of differentiated hiPSC progenies is an ongoing hurdle in clinical translation of stem cell based therapies.

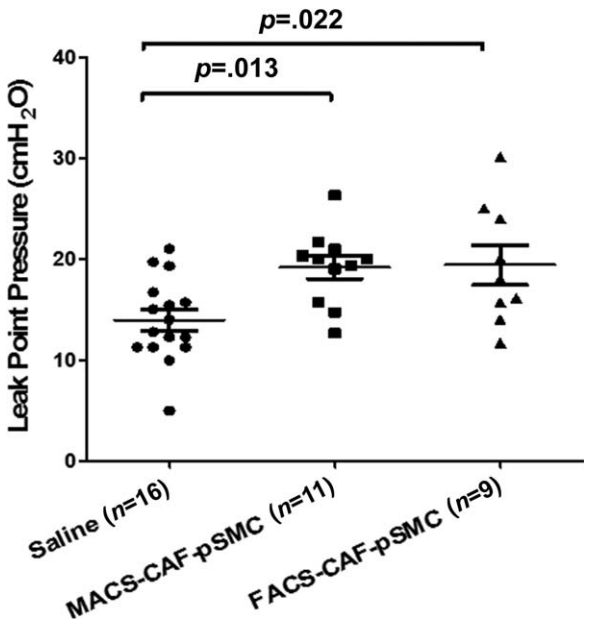


**Figure 4.** Comparison of leak point pressure (LPP) values among sham-saline, fluorescence-activated cell sorting (FACS)-sorted smooth muscle progenitor cells (pSMC) and magnetic-activated cell sorting (MACS)-sorted pSMC groups. LPP values in FACS- and MACS-sorted pSMC-treated rats were significantly higher than that in saline-treated rats. Error bar indicates mean ± standard error of mean. Abbreviations: FACS, fluorescence-activated cell sorting; LPP, leak point pressure; MACS, magnetic-activated cell sorting; pSMC, smooth muscle progenitor cells.

Despite the advances in the protocols for the differentiation of hiPSC to the committed muscle cells [25, 26, 37], induction in vitro generally result in mixed populations containing muscle cells at different development stages, cells of nonmyogenic identity and undifferentiated cells. Hence, purification or separation of the committed cells is an indispensable step in the hiPSC-based cell therapy.

A variety of cell separation methods have been reported and are now used in laboratory settings. These methods can be simply divided into two categories: separation based on physical parameters (e.g., size, density, hydrophobicity, or charge) and separation based on specific cell-surface markers. Methods based on physical parameters cannot be solely used in stem cell therapy currently due to their low purification efficiency. When higher specificity and purity is needed, higher-resolution methods based on specific cell-surface markers are applied [38]. FACS and MACS, both of which are based on cell markers, are the two most commonly investigated in current purification of hiPSC derivatives. FACS enables the separation of fluorescently labeled cells through a process that begins with laser beam illumination of a small liquid stream and offers high purification efficiencies that exceed 95% [20]. However, the throughput of FACS instruments is relatively low which limits its utility in the large-scale production of hPSC-derived cells. FACS-sorted cells often show decreased viability due to the shear stress on the cells [39]. Given these issues, FACS is not the optimal approach for autologous-hiPSC-based therapies. In contrast, MACS can be used in large scales at a throughput of $\sim 10^9$ cells for every 15 minutes [40] without the need for an experienced technician or specialized equipment, and with less damage to the cells. Hence, we explored the feasibility of MACS as a sorting technology for hiPSC-based cell therapy for the treatment of SUI.

Another critical issue concerning the purification of hiPSC derivatives is the ability to enrich or isolate a suitable intermediate cell population. Recent studies have suggested that CD34 is a general marker of progenitor cells in a variety of cell types and $CD34^+$ cells represent a distinct subset of cells with enhanced progenitor

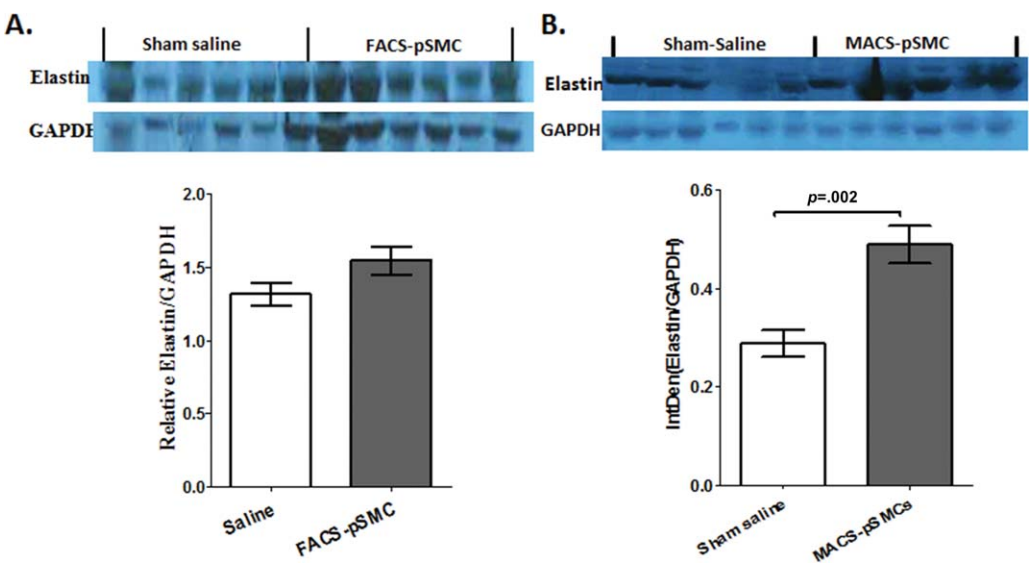


**Figure 5.** Western-blot analysis revealed an increased expression of elastin in rat bladder after magnetic-activated cell sorting (MACS)-sorted smooth muscle progenitor cells (pSMC) injection. **(A)**: Western-blot analysis of the expression of elastin protein in saline-treated and fluorescence-activated cell sorting-CAF-pSMC-treated rats. **(B)**: Western-blot analysis of elastin protein in saline-treated and MACS-CAF-pSMC-treated rats. Results were normalized with internal control GAPDH. Error bar indicates mean ± standard error of mean ($n = 6$). Abbreviations: FACS, fluorescence-activated cell sorting; MACS, magnetic-activated cell sorting; pSMC, smooth muscle progenitor cells.

activity; hence, $CD34^+$ cell subpopulation have enormous potential as cellular agents for research and for clinical cell transplantation [41, 42]. Our previous study has shown that the expression of CD34 is an extremely spatial- and temporal-dependent event during in vitro differentiation of hPSCs [25]. Thus, we selectively enriched a subpopulation of $CD34^+$ progenitors from hiPSC derivatives at a specific "time window" in the current study. These MACS-sorted $CD34^+$ cells efficiently differentiated into pSMCs as demonstrated by the expression of specific myogenic markers and down-regulated expression of genes involved in maintenance of pluripotency after in vitro directed differentiation, suggesting that MACS using cell-surface marker CD34 is a promising strategy in enriching SMC lineage-committed intermediate cell population.

Although we succeeded in induction of pSMCs from MACS-sorted $CD34^+$ cells by serial passage and directed differentiation in vitro, the derived pSMCs still contained a very low percentage of TRA-1-$60^+$ cells at passage 3. To explore the risk of these contaminated cells (especially the tumorigenic potential), we injected the derived pSMCs into SCID mice to examine long-term integration and tumor formation. Previous studies suggested that the time of in vivo tumorigenicity test using SCID mice should be roughly 12–16 weeks [43, 44]. Our previous safety experiments (manuscript in preparation), using iPSCs or hESCs, also found that teratoma formation happens at 8–12 weeks. Therefore, we set the monitoring period for 6 months after cell injection, which should be sufficient time for teratomas to appear. We observed survival of the human cells and the absence of tumor formation or abnormal histology in all of the ten SCID mice 6 months after cell transplantation. The absence of teratoma formation in our animal study is consistent with that of Schriebl et al. [45], who reported that undifferentiated hESCs can be efficiently removed using one single MACS and $1.5–4.1 \times 10^4$ contaminated hESCs detected by flow cytometry do not cause teratoma formation after transplantation. We note that safety studies with larger numbers of animals and different organ histology need to be conducted in the future to further confirm safety.

Beyond the finding that the magnetic enrichment of $CD34^+$ cells could be useful to decrease the heterogeneity and tumorigenicity of hiPSC-derived pSMCs, we also addressed the question whether MACS-sorted pSMCs are a potential source for cell therapy of SUI. Our previous study have demonstrated that periurethral injection of pSMCs derived from FACS-sorted VPCs can facilitate the structural and functional recovery of damaged urethral sphincter [27], so we compared the effect of MACS-sorted pSMCs on the SUI rat model to FACS-sorted pSMCs in this study. We demonstrated that both MACS-sorted and FACS-sorted pSMCs resulted in a similar level of urethral sphincter function recovery after local transplantation, indicating that the therapeutic effect of MACS-sorted pSMCs in not compromised by a minor degree of cell heterogeneity. A growing body of evidence suggests that, unlike traditional pharmaceutical products, strict standards for the purity of cell-based products might not be realistic and might even be undesirable in some cases in which a mixture of several cell types is necessary to achieve the desired therapeutic effect [46]. A recent study showed that after transplantation in the retina of mice, purified hiPSC-derived photoreceptors did not survive as well as nonpurified cells [47].

Abnormal ECM metabolism modulated by genetic predisposition, aging and trauma plays an essential role in the pathogenesis of SUI [48, 49]. Previous studies have observed significant changes in elastin and collagen content in the periurethral tissues of SUI women [50]. Consistent with these published data from human tissues, studies from our lab and others have showed that the protein level of elastin significantly decreased in lower urinary tract of SUI rats [28, 51]. However, after treatment with MACS-sorted pSMCs, the tissue content of elastin in the lower urinary tract significantly increased, suggesting that, in addition to cell integration, elastin deposition in the damaged rat lower urinary tract may also contribute to the therapeutic effect of MACS-sorted pSMCs.

## Summary

We have outlined an approach for purifying differentiated hiPSCs and for supplying a large-scale population of clinical-grade smooth muscle progenitors. MACS-sorted $CD34^+$ cell population can be further expanded and differentiated in vitro into specific pSMCs. These pSMCs are able to restore function and increase elastin expression of damaged urethral sphincter, comparable to the FACS-sorted derivatives in our previous study. Using MACS to enrich for desirable cells from hiPSC-derivatives and serial passaging to further reduce undifferentiated cells reduces tumorigenic risks of committed pSMCs, while still preserving therapeutic efficacy. These results may be utilized to facilitate translation of hiPSC-based cell therapy to clinical applications for treating SUI patients or other degenerative smooth muscle conditions.

## Acknowledgment

This study was supported by funding from CIRM TR3-05569.

## Author Contributions

Y.L. and M.G.: Conception and design, collection and assembly of data, data analysis and interpretation, and manuscript writing; Y.W., Y.W., P.G., and Z.W.: Collection and assembly of data, data analysis and interpretation. R.R.P.: Conception and design, provision of study material. B.C.: Conception and design, data analysis and interpretation, manuscript writing, final approval of the manuscript.

## Disclosure of Potential Conflicts of Interest

The authors indicate no potential conflicts of interest.

## References

1 Abrams P, Andersson KE, Birder L et al. Fourth International Consultation on Incontinence Recommendations of the International Scientific Committee: Evaluation and treatment of urinary incontinence, pelvic organ prolapse, and fecal incontinence. Neurourol Urodyn 2010;29:213–240.

2 Kalejaiye O, Vij M, Drake MJ. Classification of stress urinary incontinence. World J Urol 2015;33:1215–1220.

3 Hillary CJ, Osman N, Chapple C. Considerations in the modern management of stress urinary incontinence resulting from intrinsic sphincter deficiency. World J Urol 2015;33:1251–1256.

4 Bauer RM, Oelke M, Hubner W et al. [Urinary incontinence in men]. Urologe A 2015;54:887–899; quiz 900.

5 Kirchin V, Page T, Keegan PE et al. Urethral injection therapy for urinary incontinence in women. Cochrane Database Syst Rev 2012;2:Cd003881.

**6** Kenton K, Stoddard AM, Zyczynski H et al. 5-year longitudinal followup after retropubic and transobturator mid urethral slings. J Urol 2015;193:203–210.

**7** Laurikainen E, Valpas A, Aukee P et al. Five-year results of a randomized trial comparing retropubic and transobturator midurethral slings for stress incontinence. Eur Urol 2014; 65:1109–1114.

**8** Kim SO, Na HS, Kwon D et al. Bone-marrow-derived mesenchymal stem cell transplantation enhances closing pressure and leak point pressure in a female urinary incontinence rat model. Urol Int 2011;86:110–116.

**9** Lee JY, Paik SY, Yuk SH et al. Long term effects of muscle-derived stem cells on leak point pressure and closing pressure in rats with transected pudendal nerves. Mol Cells 2004;18:309–313.

**10** Silwal Gautam S, Imamura T, Ishizuka O et al. Implantation of autologous adipose-derived cells reconstructs functional urethral sphincters in rabbit cryoinjured urethra. Tissue Eng Part A 2014;20:1971–1979.

**11** Takahashi K, Tanabe K, Ohnuki M et al. Induction of pluripotent stem cells from adult human fibroblasts by defined factors. Cell 2007;131:861–872.

**12** Yu J, Vodyanik MA, Smuga-Otto K et al. Induced pluripotent stem cell lines derived from human somatic cells. Science 2007;318: 1917–1920.

**13** Reardon S, Cyranoski D. Japan stem-cell trial stirs envy. Nature 2014;513:287–288.

**14** Fox IJ, Daley GQ, Goldman SA et al. Stem cell therapy. Use of differentiated pluripotent stem cells as replacement therapy for treating disease. Science 2014;345:1247391.

**15** Okano H, Nakamura M, Yoshida K et al. Steps toward safe cell therapy using induced pluripotent stem cells. Circ Res 2013;112:523–533.

**16** Lee AS, Tang C, Rao MS et al. Tumorigenicity as a clinical hurdle for pluripotent stem cell therapies. Nat Med 2013;19:998–1004.

**17** Hentze H, Soong PL, Wang ST et al. Teratoma formation by human embryonic stem cells: Evaluation of essential parameters for future safety studies. Stem Cell Res 2009;2: 198–210.

**18** Barral S, Ecklebe J, Tomiuk S et al. Efficient neuronal in vitro and in vivo differentiation after immunomagnetic purification of mESC derived neuronal precursors. Stem Cell Res 2013;10:133–146.

**19** Xu C, Police S, Rao N et al. Characterization and enrichment of cardiomyocytes derived from human embryonic stem cells. Circ Res 2002;91:501–508.

**20** Borchin B, Chen J, Barberi T. Derivation and FACS-mediated purification of PAX3+/PAX7+ skeletal muscle precursors from human pluripotent stem cells. Stem Cell Rep 2013;1:620–631.

**21** Schuldiner M, Itskovitz-Eldor J, Benvenisty N. Selective ablation of human embryonic stem cells expressing a "suicide" gene. Stem Cells 2003;21:257–265.

**22** Koller MR, Hanania EG, Stevens J et al. High-throughput laser-mediated in situ cell purification with high purity and yield. Cytometry A 2004;61:153–161.

**23** Lim DY, Ng YH, Lee J et al. Cytotoxic antibody fragments for eliminating undifferentiated human embryonic stem cells. J Biotechnol 2011;153:77–85.

**24** Imai Y, Chou T, Tobinai K et al. Isolation and transplantation of highly purified autologous peripheral CD34+ progenitor cells: Purging efficacy, hematopoietic reconstitution in non-Hodgkin's lymphoma (NHL): Results of Japanese phase II study. Bone Marrow Transplant 2005;35:479–487.

**25** Marchand M, Anderson EK, Phadnis SM et al. Concurrent generation of functional smooth muscle and endothelial cells via a vascular progenitor. Stem Cells Transl Med 2014;3:91–97.

**26** Lian X, Bao X, Al-Ahmad A et al. Efficient differentiation of human pluripotent stem cells to endothelial progenitors via small-molecule activation of WNT signaling. Stem Cell Rep 2014;3:804–816.

**27** Wang Z, Wen Y, Li YH et al. Smooth muscle precursor cells derived from human pluripotent stem cells for treatment of stress urinary incontinence. Stem Cells Dev 2016;25: 453–461.

**28** Li Y, Wen Y, Wang Z et al. Smooth muscle progenitor cells derived from human pluripotent stem cells induce histologic changes in injured urethral sphincter. Stem Cells Transl Med 2016;5:1719–1729.

**29** Byrne JA, Nguyen HN, Reijo Pera RA. Enhanced generation of induced pluripotent stem cells from a subpopulation of human fibroblasts. PLoS One 2009;4:e7118.

**30** Wang C, Tang X, Sun X et al. TGFbeta inhibition enhances the generation of hematopoietic progenitors from human ES cell-derived hemogenic endothelial cells using a stepwise strategy. Cell Res 2012;22:194–207.

**31** Rodriguez LV, Chen S, Jack GS et al. New objective measures to quantify stress urinary incontinence in a novel durable animal model of intrinsic sphincter deficiency. Am J Physiol Regul Integr Comp Physiol 2005;288: R1332–1338.

**32** Pauwels E, De Wachter S, Wyndaele JJ. Evaluation of different techniques to create chronic urinary incontinence in the rat. BJU Int 2009;103:782–785; discussion 785–786.

**33** Herrera-Imbroda B, Lara MF, Izeta A et al. Stress urinary incontinence animal models as a tool to study cell-based regenerative therapies targeting the urethral sphincter. Adv Drug Deliv Rev 2015;82–83:106–116.

**34** Wen Y, Polan ML, Chen B. Do extracellular matrix protein expressions change with cyclic reproductive hormones in pelvic connective tissue from women with stress urinary incontinence? Hum Reprod 2006;21:1266–1273.

**35** Kitajima Y, Doi H, Ono Y et al. Estrogen deficiency heterogeneously affects tissue specific stem cells in mice. Sci Rep 2015;5:12861.

**36** Conway DA, Kamo I, Yoshimura N et al. Comparison of leak point pressure methods in an animal model of stress urinary incontinence. Int Urogynecol J Pelvic Floor Dysfunct 2005;16:359–363.

**37** Patsch C, Challet-Meylan L, Thoma EC et al. Generation of vascular endothelial and smooth muscle cells from human pluripotent stem cells. Nat Cell Biol 2015;17:994–1003.

**38** Rodrigues GM, Rodrigues CA, Fernandes TG et al. Clinical-scale purification of pluripotent stem cell derivatives for cell-based therapies. Biotechnol J 2015;10:1103–1114.

**39** Fernandes TG, Rodrigues CA, Diogo MM et al. Stem cell bioprocessing for regenerative medicine. J Chem Technol Biotechnol 2014;89:34–47.

**40** Miltenyi S, Muller W, Weichel W et al. High gradient magnetic cell separation with MACS. Cytometry 1990;11:231–238.

**41** Sidney LE, Branch MJ, Dunphy SE et al. Concise review: Evidence for CD34 as a common marker for diverse progenitors. Stem Cells 2014;32:1380–1389.

**42** Shi Q, VandeBerg JL. Experimental approaches to derive CD34+ progenitors from human and nonhuman primate embryonic stem cells. Am J Stem Cells 2015;4:32–37.

**43** Kanemura H, Go MJ, Shikamura M et al. Tumorigenicity studies of induced pluripotent stem cell (iPSC)-derived retinal pigment epithelium (RPE) for the treatment of age-related macular degeneration. PLoS One 2014;9: e85336.

**44** Kuroda T, Yasuda S, Sato Y. Tumorigenicity studies for human pluripotent stem cell-derived products. Biol Pharm Bull 2013;36: 189–192.

**45** Schriebl K, Satianegara G, Hwang A et al. Selective removal of undifferentiated human embryonic stem cells using magnetic activated cell sorting followed by a cytotoxic antibody. Tissue Eng Part A 2012;18:899–909.

**46** Serra M, Brito C, Correia C et al. Process engineering of human pluripotent stem cells for clinical application. Trends Biotechnol 2012;30:350–359.

**47** Lamba DA, McUsic A, Hirata RK et al. Generation, purification and transplantation of photoreceptors derived from human induced pluripotent stem cells. PLoS One 2010;5:e8763.

**48** Chen B, Yeh J. Alterations in connective tissue metabolism in stress incontinence and prolapse. J Urol 2011;186:1768–1772.

**49** Campeau L, Gorbachinsky I, Badlani GH et al. Pelvic floor disorders: Linking genetic risk factors to biochemical changes. BJU Int 2011;108:1240–1247.

**50** Goepel C, Thomssen C. Changes in the extracellular matrix in periurethral tissue of women with stress urinary incontinence. Acta Histochem 2006;108:441–445.

**51** Dissaranan C, Cruz MA, Kiedrowski MJ et al. Rat mesenchymal stem cell secretome promotes elastogenesis and facilitates recovery from simulated childbirth injury. Cell Transplant 2014;23:1395–1406.

See www.StemCellsTM.com for supporting information available online.